EUROfusion

WPMAT-PR(18) 21318

S Novak et al.

The beneficial effects of WC addition in FAST-densified tungsten

Preprint of Paper to be submitted for publication in
Journal of Nuclear Materials

This work has been carried out within the framework of the EUROfusion Consortium and has received funding from the Euratom research and training programme 2014-2018 under grant agreement No 633053. The views and opinions expressed herein do not necessarily reflect those of the European Commission.

The beneficial effects of WC addition in FAST-densified tungsten

Saša Novak [1], Matej Kocen [1,2], Andreja Šestan Zavašnik[2,3], Andrei Galatanu[4], Magdalena Galatanu[4], Elena Marija Tejado Garrido [5], Ignacio Pastor[5], Petra Jenuš [1]

[1] Dept. for Nanostructured Material, Jožef Stefan Institute, Ljubljana, Slovenia
[2] Jožef Stefan International Postgraduate School, Ljubljana, Slovenia
[3] Center for Electron Microscopy, Jožef Stefan Institute, Ljubljana, Slovenia
[4] National Institute of Materials Physics, Magurele, Romania
[5] Polytechnic University of Madrid, Madrid, Spain

Corresponding author: Saša Novak (sasa.novak@ijs.si)

ABSTRACT

Dispersion-strengthening of fusion-relevant tungsten by incorporation of tungsten sub-carbide W_2C particles on grain boundaries is demonstrated as an effective way to eliminate detrimental W-oxide, enhance densification and to stabilise the composite's microstructure and flexural strength at the room as well as high temperatures. The W_2C particles are formed *in situ* during sintering by carbon diffusion from WC-nanoparticles added as a precursor into W-matrix. Even in extremely fast sintering process using Field-Assisted-Sintering-Technology (FAST, 1900°C, 5 min), the added WC completely transform to W_2C resulting in W-W_2C composite. While at least 5 vol. % of WC nanoparticles are needed for elimination of the oxide, approximately 10 vol. % result in a W-W2C composition with favourable characteristics.

Keywords:

fusion, tungsten, carbide, dispersion-strengthening, WC, W_2C, Field-Assisted-Sintering-Technology (FAST)

Highlights:

- Addition of submicron WC powder to tungsten powder promotes its densification and results in the reduced presence of oxide in tungsten-based materials.
- Further addition of WC leads to the formation of W_2C particles on W-grain boundaries thus stabilising the microstructure at high temperatures
- W-W_2C composites prepared with 10 vol. % WC exhibit improved mechanical properties in comparison with W and similar thermal conductivity.

The beneficial effects of WC addition in FAST-densified tungsten

ABSTRACT

Dispersion-strengthening of fusion-relevant tungsten by incorporation of tungsten sub-carbide W_2C particles on grain boundaries is demonstrated as an effective way to eliminate detrimental W-oxide, enhance densification and to stabilise the composite's microstructure and flexural strength at the room as well as high temperatures. The W_2C particles are formed *in situ* during sintering by carbon diffusion from WC-nanoparticles added as a precursor into W-matrix. Even in extremely fast sintering process using Field-Assisted-Sintering-Technology (FAST, 1900°C, 5 min), the added WC completely transform to W_2C resulting in W-W_2C composite. While at least 5 vol. % of WC nanoparticles are needed for elimination of the oxide, approximately 10 vol. % result in a W-W2C composition with favourable characteristics.

1. INTRODUCTION

Development and implementation of fusion power plants promise a significant contribution to the clean and safe energy supply for future generations. To assure their high efficiency and safe operation, large efforts are put into the development of suitable structural materials capable of withstanding the extreme conditions in the reactor. Within the DEMO design, one of the important tasks is to select a suitable material for the divertor, which is the key in-vessel component. Divertor is responsible for heat transfer and impurity removal via guided plasma exhaust and is therefore subjected to very high heat-fluxes. Although in the last decades, the progress in the field of fusion-relevant materials has been substantial, development of low-activation materials capable of withstanding high-heat-loads of more than 10 MW/m^2, with sufficient mechanical and thermal properties, which are retained even after high neutron irradiation dose and nuclear transmutations, remains among the priorities of the fusion research programmes [1-3].

Current research focuses on the development of tungsten-based materials. In contrast to some attractive thermo-physical properties of the tungsten [4], its properties deteriorate under operational conditions. Namely, ductile-to-brittle-transition (DBT) in the temperature range around 400 °C as well as the recovery, recrystallization and exaggerated grain growth at temperatures above 1000 °C, are obstacles for the use of pure tungsten in the proposed operational window of the DEMO reactor [1, 4, 5].

Among the currently proposed solutions for structural stabilisation of tungsten is dispersion-strengthening by incorporation of oxide- (e.g. Y_2O_3) or carbide- (e.g. TiC, TaC) based particles into W-matrix which were demonstrated to improve the material's mechanical properties to a certain extent [6] [7-10]. As an alternative, we recently proposed reinforcement of the tungsten with W_2C particles, synthesized *in situ* during sintering by reaction of a carbide precursor [11, 12]. Various precursors were verified: graphene, phenol-formaldehyde resin and WC nanoparticles. It was confirmed that during pressure-less sintering at 2200 °C in vacuum furnace all three precursors resulted in the formation of W_2C inclusions but only in the case of WC addition no carbonaceous residues were found. Therefore, WC nanoparticles were suggested as the most suitable precursor.

This work aimed to verify the formation of W_2C particles at the W-grain boundaries during sintering by Field-Assisted-Sintering-Technology (FAST) an advanced consolidation technique, capable to efficiently densify materials in a very short time and at a lower temperature in comparison with conventional sintering. The WC nanoparticles were used as a precursor for W_2C inclusions. Special attention was paid to the phase composition after the FAST-sintering, in particular to the presence of W_2C and oxides. The effect of inclusions on mechanical properties and the thermal conductivity was analysed from room temperature to 1200 °C. The effect of ageing during 24 hours of heating at 1600 °C on the microstructure and mechanical properties was also verified.

2. EXPERIMENTAL

2.1 Samples preparation

Tungsten powder with an average grain size of ≤ 1.5 µm (Global Tungsten & Powders spol. S r.o., Czech Republic) was used in this study. According to the producer's specification, the oxygen content in the powder was 0.105 wt. %. i.e. 1.2 at. %. The tungsten powder was mixed with WC powder (150-200 nm, >99 %, Aldrich, Germany) in cyclohexane (Sigma Aldrich, Germany) and homogenised by an ultrasonic finger for 3 minutes at a power of 50 % and amplitude 1 s^{-1}. The suspensions were then freeze-dried to prevent oxidation and separation of the phases with different specific weight. The powder mixtures with compositions presented in Table 1 were sintered in graphite dye with an inner diameter of 16 mm by field assisted sintering (FAST, Dr. Sinter FAST 515-S, Sumimoto FAST Syntex Ltd., Japan) at 1900 °C with a heating rate of 100 °/min, for 5 min and applied pressure of 60 MPa. Before FAST processing, the reaction chamber was purged several times with high purity argon and evacuated again. During sintering, the pressure inside the chamber was below 10 Pa. For comparison, pure tungsten (sample W) was sintered in a high-temperature vacuum furnace with

graphite heating elements (Thermal Technology, USA) at 2200 °C for 6 h. Additionally, the sintered samples were aged at 1600 °C for 24 hours in vacuum.

Table 1: Samples composition

Sample	The composition of the powder mixtures (vol. %)	Conc. of carbon in the starting mixture (at. %)
W	W	0
W-1WC	99.2 W + 1WC	0.75
W-5WC	95 W + 5 WC	3.7
W-10WC	90 W + 10 WC	7.2
W-25WC	75 W + 25 WC	16.7

2.2 Characterisation

Before the analysis, we removed the outer, carbon contaminated, layer of the sintered material by grinding. The phase composition of sintered samples was analysed by X-ray diffraction (XRD; AXS U8, Bruker Co., USA) utilizing CuKα radiation at room temperature (step width of 0.02°, fixed time of 1 s, a scanning range of 2θ = 20° to 80°). Rietveld analysis was performed by programme package Topas, Bruker AXS, Karlsruhe, Germany.

The microstructure of the samples before and after high-temperature ageing was characterised by scanning electron microscopy (FE-SEM, JSM-7600F, Jeol Inc., Japan). For the detection and identification of the secondary phase electron backscattered diffraction mapping (EBSD; HKL Channel 5, Oxford Instruments plc, UK) was performed.

Mechanical properties of as-sintered and aged (1600°C for 24h) samples were evaluated at room temperature by ball-on-three-balls flexural strength test. Three samples per composition were tested.

High-temperature flexural strength was measured in vacuum (10^{-6}mBar) in the temperature range from RT to 1200 °C by three-point-bending test (TPB). The heating rate was 10°C/min with 10 minutes hold; crosshead speed was 100 µm/min, the sample size was 2x2x20 mm^3. Fracture toughness was measured by TPB test on pre-notched samples (femto-laser notch).

The thermal transport properties were investigated using a Netzsch LFA 457 Microflash up to 1000 °C. The LFA equipment allows the direct measurement of the thermal diffusivity, while the specific heat of the materials was determined by a differential method using a Molybdenum_SRM781 standard sample as a reference. The thermal conductivity was calculated by $\lambda = \alpha \times \rho \times Cp$, with ρ the density, C_p the specific heat and α the thermal diffusivity of the material. The samples' density was measured by the Archimedes method using a high-resolution balance. Several measurements (up to five per material) have been performed for each material.

3. RESULTS

3.1 The composition of the as-sintered samples

Table 2 summarizes the expected (calculated from starting powder composition) and measured content of W_2C in the samples prepared by various WC powder addition and sintered by FAST. The W_2C content was determined by Rietveld refinement analysis of experimental XRD spectra using least squares methods.

Table 2: Content of W_2C in W-W_2C composite samples as calculated and analysed by XRD

Sample	Calculated content of W_2C (wt. %)	Content of W_2C as determined by Rietveld refinement analysis (wt. %)
W	0	-
W-1WC	1.6	(*)
W-5WC	8	(*)
W-10WC	16	4
W-25WC	41	30

(*) below detection limit (< 3 wt. %)

As presented in Table 2 and illustrated in Figure 1, in the sample with the addition of 1 vol. % of WC (W-1WC) no W_2C was detected by XRD analysis. The same result was also obtained for the W-5WC where, according to calculation, the expected W_2C content was 8 wt. %. This was ascribed to the content below the detection limit of the laboratory XRD. At larger additions of WC nanoparticles as a source of carbon, the peaks in XRD spectra confirm the presence of W_2C secondary phase.

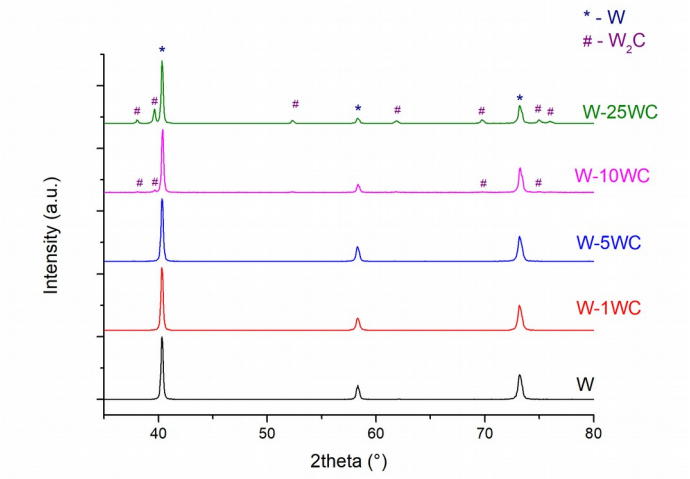

Figure 1: XRD spectra of the tungsten-based samples with increasing addition of WC in starting composition.

3.2 The microstructure of the as-sintered samples

Figures 2a-2e illustrate the characteristic fracture surfaces of the examined samples sintered by FAST for five minutes at 1900 °C. For comparison, a microstructure of the pure tungsten sample sintered in

the high-temperature vacuum furnace at 2200 °C for 6 h is presented in Figure 2aa. Densification by FAST resulted in finer microstructure and much lower porosity when compared to the conventional sintering (Figures 2a and 2aa, respectively). An important feature observed in the FAST-sintered tungsten is the presence of small, liquid-like, inclusions on grain boundaries (inset in Figure 2a), while in conventionally sintered tungsten such inclusions were not observed. According to the results of our previous study [13], similar inclusions in the FAST-densified tungsten are monoclinic tungsten dioxide WO_2. As its melting point (1700 °C) is below the sintering temperature by FAST (1900 °C), we assume that the specific neck-shaped morphology of the observed inclusions results from melting during sintering. Furthermore, this study also revealed that during prolonged heating at high temperature, the oxide evaporates leaving voids and blisters behind (see Figure 8b).

a: W (FAST)

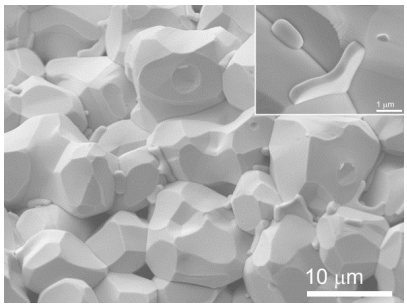

aa: W (vacuum sintered @2200 °C)

b: W-1WC (FAST)

c: W-5WC (FAST)

d: W-10WC (FAST)

e: W-25WC (FAST)

Figure 2: Fracture surfaces of the samples W (a), W-1WC (b), W-5WC (c) W-10WC (d) and W-25WC (e), densified by FAST. A tungsten sample sintered in high-temperature vacuum furnace is presented for comparison (aa). Inset in Fig. 2a: Secondary phase in the tungsten sample densified by FAST

Similarly to the FAST-sintered sample W, the sample W-1WC reveals the presence of neck-shaped oxide inclusions at the W grain boundaries (Figure 2b), while only a few such inclusions were observed in the microstructure of the sample with 5 vol. % WC addition (W-5WC, Figure 4c). This suggests that the majority of the present oxygen was consumed by carbon from the WC particles leaving pure tungsten behind. The oxide inclusions were also not observed for the samples with 10 or 25 vol. % WC addition (Figure 2d and 2e, respectively). We assume that the carbon content was sufficiently high to consume all the present oxygen to form volatile products.

Moreover, the microstructures of the samples W-10WC (Figure 2d) and W-25WC (Figure 2e) reveal smaller grains than observed for the samples W, W-1WC and W-5WC. One can observe small inclusions with different morphology than observed for the W and W-1WC. According to the results of XRD analysis (see Table 2 and Figure 1) these inclusions are hexagonal W_2C grains formed from WC after losing a part of carbon. As evident, by the addition of WC in the starting mixture, the transgranular fracture mode is promoted.

Differentiation between the W and W_2C by conventional backscattered electron (BSE-SEM) technique is, unfortunately, impossible due to the strong channelling effect, produced by random orientation of the W grains. The orientational contrast prevails over the small difference in Z-number between W and W_2C. Thus, for identification of the phases, we employed EBSD, which enabled to distinguish between both phases regarding their crystal structure instead of their chemical composition. The EBSD analysis confirmed the presence of small W_2C inclusions on the W grain boundaries of the samples W-10WC (Figure 3a) and W-25WC (Figure 3b).

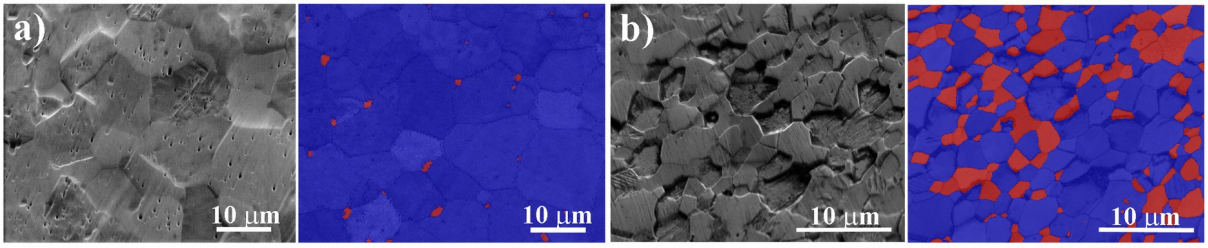

Figure 3: Secondary electrons SEM image with the corresponding EBSD map of the phases present in the sample W-10WC (a) and sample W-25WC (b). Two distinct phases can be seen: blue represents the W-matrix and red represents the W_2C inclusions.

3.3 Mechanical properties at room and elevated temperature

As illustrated in Figure 4, the density of the FAST-sintered W-based materials increases with the increased WC addition and reaches above 99 % of theoretical density with 25 vol. % WC addition. Accordingly, the flexural strength also increases up to 10 vol. % (sample W-10WC). This is in accordance with the microstructures presented in Figure 2, which suggested that the addition of 10 vol. % WC or more assures absence of the oxide phase and enables the formation of W_2C particles at the tungsten grain boundaries.

To verify the effect of the W_2C inclusions on the tungsten grain growth at high temperatures (such as possible boundary conditions in the DEMO device), we aged the sintered samples at 1600 °C for 24 hours. As illustrated by dark bars in Figure 4, during ageing the flexural strength degrades for all the examined samples.

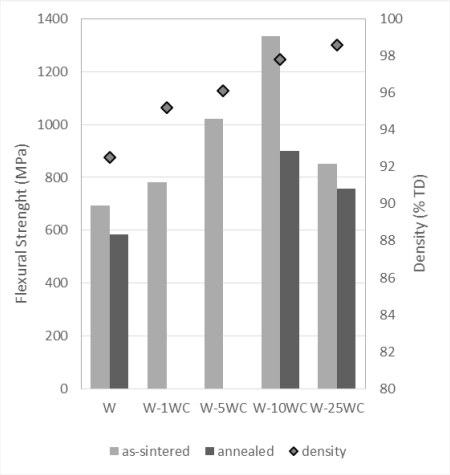

Figure 4: Room temperature flexural strength of the samples after sintering and after ageing for 24 hours at 1600 °C

The sample W-10WC and W as a reference were further analysed for the flexural strength during heating in vacuum. Figure 5 shows that ultimate flexural strength (solid lines) for the W-10WC increases up to 800 °C (~1500 MPa), where it starts to descend. As the stress-strain curves in Figures 6a and 6b imply that brittle fracture prevails only up to 400 °C for both W and W-10WC, above this temperature flexural yield strength (at 0.2 % strain) is plotted by the dashed line. As evident, the values for W-10WC are much higher than those for the FAST-densified tungsten (W), for which the strength gradually decrease from 680 MPa at room temperature to 300 MPa at 1000 °C. From the diagrams in Figures 6c and 6d, it is also evident that not only the stress is significantly higher for the W-10WC but also the deformation.

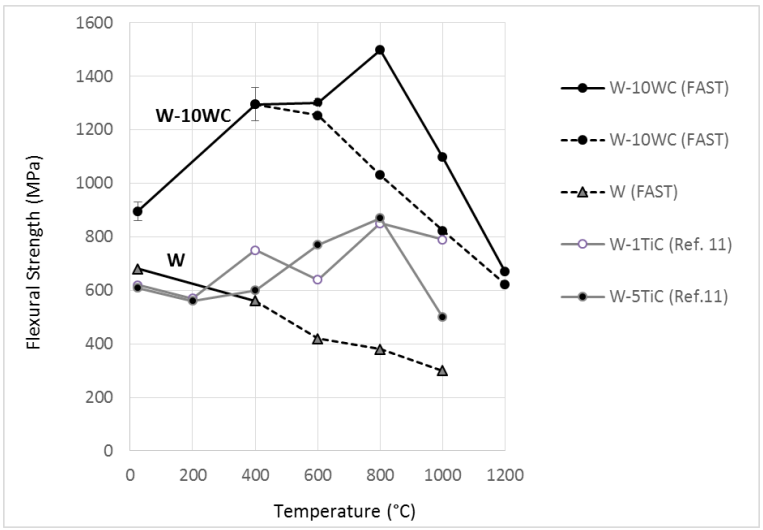

Figure 5: Flexural strength of FAST densified samples W and W-10WC as a function of temperature - solid lines: Ultimate flexural strength; dashed lines: flexural yield strength (at 0.2 % strain)

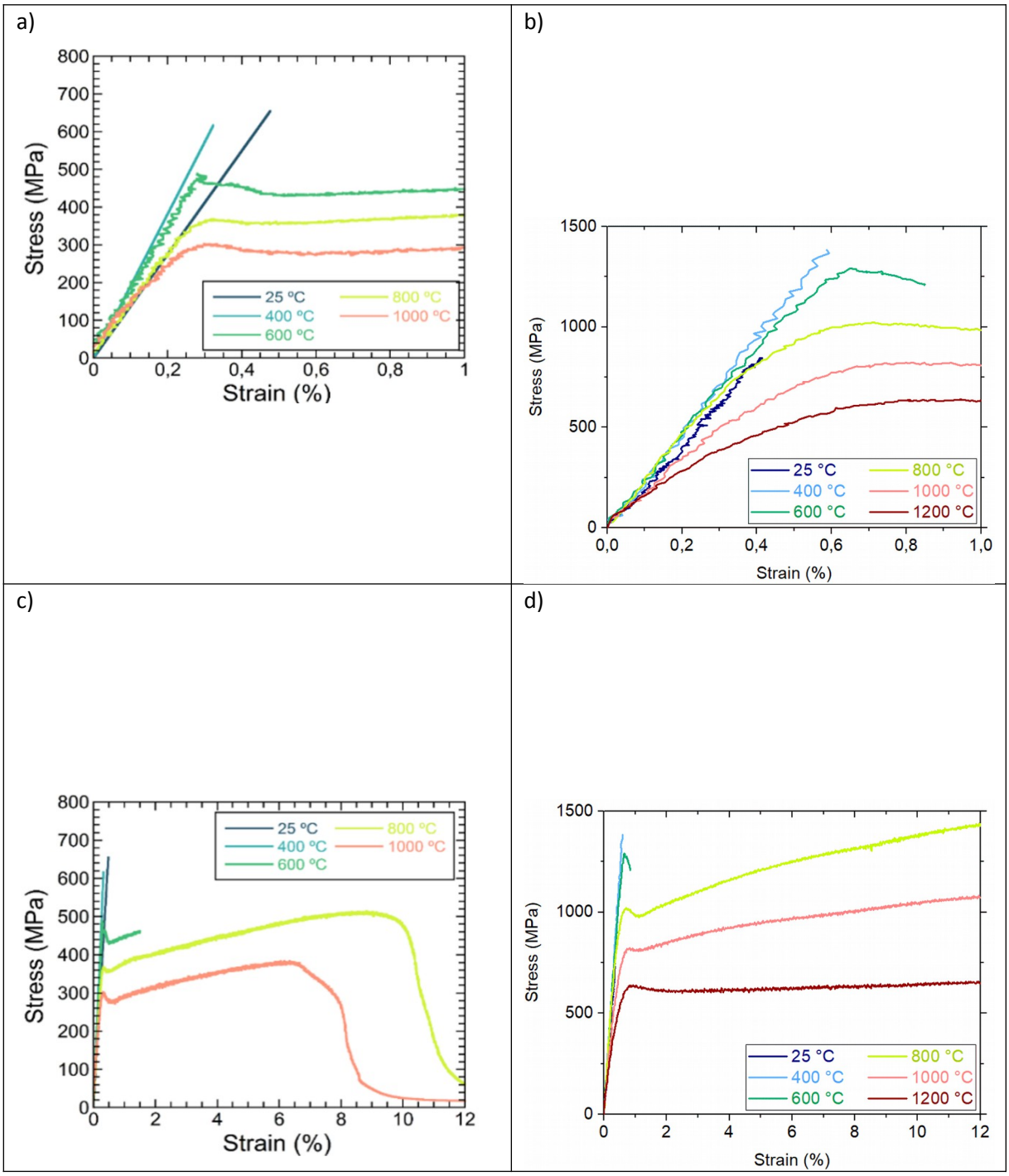

Figure 6: Stress-strain curves for FAST-densified W (a, c) and W-10WC (b, d)

As illustrated in Figure 7, the fracture toughness of the W-W10WC gradually increases with temperature up to 1000 °C. Brittle behaviour is suggested up to 800 °C.

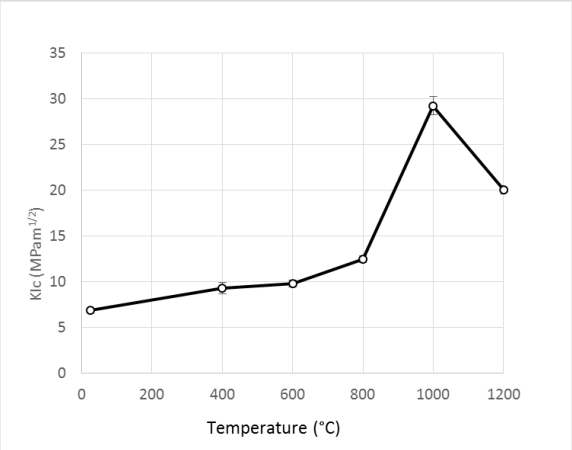

Figure 7: Fracture toughness of the composite W-10WC as a function of temperature

3.4 Ageing at high temperature

Figures 8a-d illustrate the effect of ageing at 1600 °C for 14 h on the microstructure of W and W-10WC samples. The comparison of Figures 8a and b reveals slightly larger W grains after ageing. We suppose that the WO_2 inclusions act similarly as carbide or oxide inclusions, i.e. they inhibit tungsten grain growth. However, during prolonged heating, the inclusions evaporate due to the low melting point that enables the growth of W grains. This assumption is supported by the microstructure in Figure 8b, which reveals the absence of oxide inclusions. On the contrary, the W_2C inclusions at the tungsten grain boundaries in the sample W-10WC are stable at these conditions (1600 °C, 24 hours), which results in a nearly unchanged microstructure after ageing (Figure c and d).

a) W as sintered (before ageing)	b) W after ageing at 1600 °C, 24 h
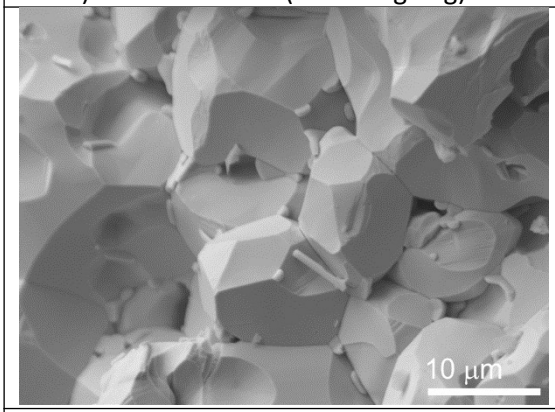	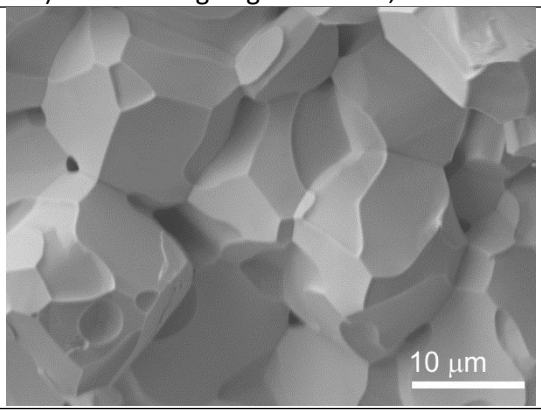
c) W-10WC as sintered (before ageing)	d) W-10WC after ageing at 1600 °C, 24 h

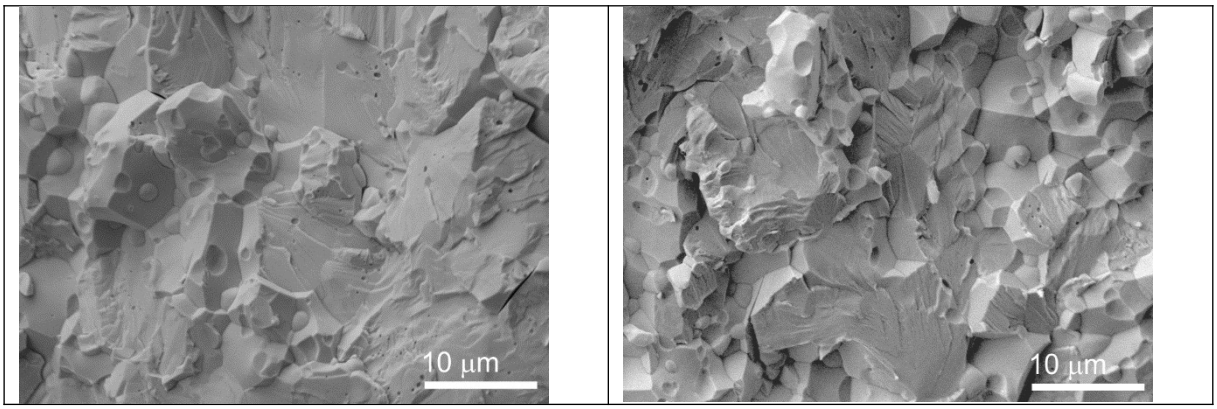

Figure 8: Fracture surfaces (SEM) of the FAST densified samples W and W-10WC before (a and c, respectively) and after ageing (b and d, respectively) at 1600 °C for 24 hours

3.5 Thermal conductivity

The thermal conductivity of up to five samples each from W and W-10WC was measured during heating up to 1000 °C. The mean values obtained are presented in Fig. 9. As evident, the W-10WC exhibits slightly lower thermal conductivity at moderate temperatures as compared to W. Note that the FAST-densified tungsten has slightly lower conductivity as compared to the ITER grade W [14] due to its lower density and presence of WO_2.

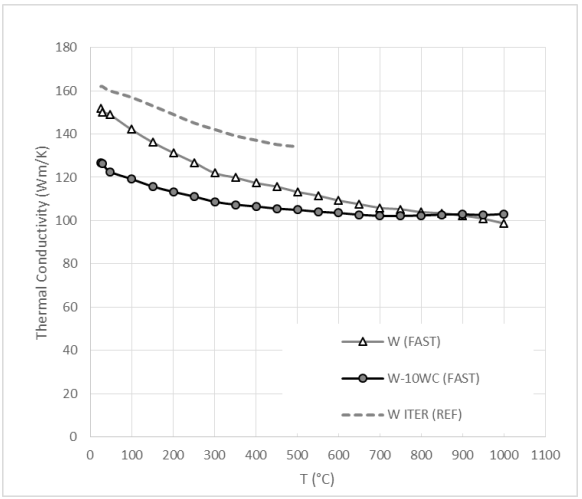

Figure 9: Mean thermal conductivity values for the FAST-densified W and W-10WC samples in comparison with W ITER [14]

4. DISCUSSION

The Field-Assisted-Sintering Technology (FAST) has opened a new horizon in sintering of refractory materials including tungsten. This was proven very effective technique for rapid densification of pure and doped tungsten [15]. However, as the tungsten powder usually contains an oxide layer on the

surface [16, 17], presence of oxides appears more problematic than in the conventional sintering. In conventional sintering, hydrogen atmosphere is used as a quite efficient reducing agent, but it is not applicable in FAST as densification is driven by pulsed electric current. Due to the extremely high heating rate, it seems that there is not enough time for the formation and evaporation of gaseous products. As an alternative, the carbon could be added but is related to the possible presence of unwanted residual free carbon [11]. Thus, the addition of "sacrificial" phase such as WC, capable to "donate" the needed amount of carbon for the reaction with oxygen, while leaving only tungsten behind, appears a favourable option. As presented in this work, at least 5 vol. % of WC addition is needed for the elimination of the WO_2 from the tungsten grains, which beneficially affects the density and flexural strength of tungsten (see Figure 4). It has to be taken into account, however, that decarburization of WC during sintering depends directly on the content and nature of oxygen in the starting powders [17].

Moreover, as it is presented in this work, larger addition of submicron WC powder to tungsten beneficially affects the microstructure and mechanical properties of the material. XRD and EBSD analysis confirmed that W_2C is formed during FAST-densification of W-WC mixtures. This is in agreement with the W-C phase diagram showing WC and W_2C the only stable phases in the temperature range of sintering [18]. The W_2C particles formed by decarburisation of the WC nanoparticles within the W matrix pin the grain boundaries to prevent tungsten grain growth at high temperatures. A similar effect was also observed for pores, Y_2O_3, TiC and TaC inclusions [7, 19]. However, oxide inclusions may degrade thermal conductivity, while TiC and TaC form mixed carbides $(W,Ti)C_{1-x}$ and $(W,Ta)_{1-x}$ in a wide range of composition that might lead to the growth of the carbide particles after prolonged heating.

The W-W_2C composites reflect significantly improved density and mechanical properties at room as well as at high temperatures. Favourable characteristics were observed in particular for the sample prepared with 10 vol. % of WC addition. The addition of WC to the W-matrix also promote transgranular fracture mode (see Figure 8) that suggests cleaner and stronger grain boundaries. We assume that this is mainly the consequence of the absence of oxide phase, but obviously, despite considered as a brittle phase, the W_2C beneficially affect the strength.

As presented in Figures 5 and 6, the flexural strength is much higher in comparison with the tungsten within the wide range of temperatures up to 1200 °C and larger plastic deformation is enabled. The obtained flexural strength for W-10WC is also significantly higher in comparison with the values for W-1TiC and W-5TiC measured by the same technique and reported by Tejado [9]. Furthermore, the composites W-1TiC and W-5TiC exhibit the onset of plastic deformation at a higher temperature, i.e.

at 1200°C and 1000°C, respectively [9], while in the case of W-10WC this was observed already at 600 °C (see Figure 6). Overall, when the flexural strength for the W-10WC is compared with literature data for the temperature-related strength of dispersion-strengthen W containing TiC, TaC or Y_2O_3 [20] [21], the W_2C inclusions seem to have the most advantageous effect.

The observed relatively low flexural strength of the FAST-densified W could be ascribed to the high porosity and presence of oxide inclusions (see Figure 2a). For comparison, most of the values for pure polycrystalline tungsten reported within the last decade suggest the room temperature strength up to 600 MPa and its decrease with temperatures. Much higher values were reported only for the rolled tungsten produced by Plansee, reaching 1500 MPa at 800 °C [9].

The fracture toughness of the W-10WC is a bit lower in comparison with the W-1TiC and W-5TiC reported by Tejado [9] and similar to the Charpy toughness reported by Reiser at al [22]. Literature data for polycrystalline tungsten implies the brittle-to-ductile transition at around 400 °C [2]. For the W-10WC, the peak value (~30 $MPm^{1/2}$) was observed at 1000 °C.

While there are many literature data on flexural strength and ductility of pure and dispersion strengthened tungsten as a function of temperature, the data on the effect of high-temperature ageing on mechanical properties is very scarce. For example, Reiser et all [22] analysed the toughness of W plate in a wide range of temperatures after prolonged ageing and found that the Charpy toughness abruptly decreases after 1000 hours. Massive degradation of mechanical properties at 600 °C was also observed for mechanically alloyed and subsequently hot isostatically pressed W with Y_2O_3 [23]. On the other hand, the results of this study reveal that ageing at 1600 °C for 24 hours negligibly affected the microstructure of W-10WC and a decrease in the flexural strength from 1330 MPa to 900 MPa.

5. CONCLUSIONS

Here we present dispersion strengthening of tungsten achieved by incorporation of WC nanoparticles as a precursor for the W_2C inclusions. The W_2C particles are formed at the tungsten grain boundaries during densification by carbon diffusion from WC-particles. After densification by FAST at 1900°C, 5 min, two phases are detected in the sintered composite: cubic W and hexagonal W_2C, which implies the complete transformation of the WC. No oxide was detected in the W-W_2C composites in contrast to FAST-densified pure tungsten, where the oxide phase was found on the W-grain boundaries.

The addition of at least 5 vol. % of the submicron WC has successfully prevented oxidation of W, while larger amounts contributed to the beneficial formation of the desired carbide particle W_2C, which inhibit tungsten grain growth during ageing at high temperatures. The composite with the addition of approximately 10 vol. % WC inclusions (sample W-10WC) reflects the highest flexural

strength at RT (>1300 MPa) as well as at elevated temperatures, with the onset of plastic deformation at 600 °C. Moreover, high-temperature thermal conductivity is relatively high and remains above 100 Wm/K up to 1000 °C.

ACKNOWLEDGEMENT

This work has been carried out within the framework of the EUROfusion Consortium and has received funding from the Euratom research and training programme 2014-2018 under grant agreement No 633053. The views and opinions expressed herein do not necessarily reflect those of the European Commission. Parts of the work have been performed within the PhD studies of Mrs Andreja Šestan Zavašnik and Mr Matej Kocen; both supported within the Eurofusion education & training scheme. This project has received funding from Slovenian Research Agency (Contract No. 1000-17-0106, J2-8165). The authors also acknowledge the support of the Ministerio de Economía y Competitividad of Spain (research project MAT2015-70780-C4-4-P) and the Comunidad de Madrid (research project S2013/MIT-2862-MULTIMATCHALLENGE) who have funded this research.

DATA AVAILABILITY STATEMENT

Data are available upon request.

REFERENCES

1. Rieth, M., et al., *Review on the EFDA programme on tungsten materials technology and science.* Journal of Nuclear Materials, 2011. **417**(1-3): p. 463-467.
2. Rieth, M., et al., *Recent progress in research on tungsten materials for nuclear fusion applications in Europe.* Journal of Nuclear Materials, 2013. **432**(1-3): p. 482-500.
3. Rowcliffe, A.F., et al., *Materials-engineering challenges for the fusion core and lifetime components of the fusion nuclear science facility.* Nuclear Materials and Energy, 2018. **16**: p. 82-87.
4. Norajitra, P., *Divertor development for a future fusion power plant*. 2014: KIT Scientific Publishing.
5. Gumbsch, P., et al., *Controlling factors for the brittle-to-ductile transition in tungsten single crystals.* Science, 1998. **282**(5392): p. 1293-1295.
6. Kim, Y., et al., *Fabrication of high temperature oxides dispersion strengthened tungsten composites by spark plasma sintering process.* International Journal of Refractory Metals and Hard Materials, 2009. **27**(5): p. 842-846.
7. Kitsunai, Y., et al., *Microstructure and impact properties of ultra-fine grained tungsten alloys dispersed with TiC.* Journal of Nuclear Materials, 1999. **271**: p. 423-428.
8. Lang, S., et al., *Microstructure, basic thermal–mechanical and Charpy impact properties of W-0.1 wt.% TiC alloy via chemical method.* Journal of Alloys and Compounds, 2016. **660**: p. 184-192.
9. Garrido, E.M.T., *Performance of structural materials for the DEMO divertor*. 2017, Universidad Politécnica de Madrid.
10. Antusch, S., et al., *Mechanical and microstructural investigations of tungsten and doped tungsten materials produced via powder injection molding.* Nuclear Materials and Energy, 2015. **3-4**: p. 22-31.

11. Jenuš, P.I., A.; Kocen, M.; Šestan, A.; Novak, S. , *W2C-reinforced tungsten prepared by use of different precursors.* Ceramics International (submitted), 2018.
12. Jenuš, P.I., A.; Kocen, M.; Šestan, A.; Zavasnik, J.; Novak, S., *W2C-reinforced W prepared with in-situ synthesis of W2C nanoparticles from various carbon source* in *13th International Symposium on Fusion Nuclear Technology, ISFNT-13*. 2017: Kyoto.
13. Sestan, A., et al., *The role of tungsten phases formation during tungsten metal powder consolidation by FAST: Implications for high-temperature applications.* Materials Characterization, 2018. **138**: p. 308-314.
14. Miao, S., et al., *Mechanical properties and thermal stability of rolled W-0.5 wt% TiC alloys.* Materials Science and Engineering a-Structural Materials Properties Microstructure and Processing, 2016. **671**: p. 87-95.
15. Autissier, E., et al., *Spark plasma sintering of pure and doped tungsten as plasma facing material.* Physica Scripta, 2014. **T159**.
16. Šestan, A., *Identification of phases formed during field assisted sintering of tungsten.*
17. Kurlov, A.S., *Effects of vacuum annealing on the particle size and phase composition of nanocrystalline tungsten carbide powders.* Russian Journal of Physical Chemistry A, 2013. **87**(4): p. 654-661.
18. Kurlov, A. and A. Gusev, *Tungsten carbides and WC phase diagram.* Inorganic Materials, 2006. **42**(2): p. 121-127.
19. Worner, C.H. and P.M. Hazzledine, *GRAIN-GROWTH STAGNATION BY INCLUSIONS OR PORES.* Jom-Journal of the Minerals Metals & Materials Society, 1992. **44**(9): p. 16-20.
20. Song, G.M., Y. Zhou, and Y.J. Wang, *The microstructure and elevated temperature strength of tungsten-titanium carbide composite.* Journal of Materials Science, 2002. **37**(16): p. 3541-3548.
21. Lukac, F., et al., *Properties of Mechanically Alloyed W-Ti Materials with Dual Phase Particle Dispersion.* Metals, 2017. **7**(1).
22. Reiser, J., et al., *Ductilisation of tungsten (W): On the increase of strength AND room-temperature tensile ductility through cold-rolling.* International Journal of Refractory Metals & Hard Materials, 2017. **64**: p. 261-278.
23. Palacios, T., et al., *Mechanical characterisation of tungsten-1 wt.% yttrium oxide as a function of temperature and atmosphere.* Journal of Nuclear Materials, 2014. **454**(1-3): p. 455-461.